AIMS Geosciences

AIMS Geosciences, 10(4): 662–683.
DOI: 10.3934/geosci.2024034
Received: 31 May 2024
Revised: 29 July 2024
Accepted: 13 August 2024
Published: 04 September 2024

http://www.aimspress.com/journal/geosciences

Research article

Artificial intelligence and 3D subsurface interpretation for bright spot and channel detections

Yasir Bashir[1,*], Muhammad Afiq Aiman Bin Zahari[2], Abdullah Karaman[1], Doğa Doğan[1], Zeynep Döner[3], Ali Mohammadi[4], and Syed Haroon Ali[5]

[1] Department of Geophysical Engineering, Faculty of Mines, İstanbul Technical University, İstanbul, Türkiye
[2] Faculty of Science, Universiti Teknologi Malaysia (UTM), Johor Bahru, Malaysia
[3] Department of Geological Engineering, Faculty of Mines, İstanbul Technical University, İstanbul, Türkiye
[4] Eurasia Institute of Earth Sciences, İstanbul Technical University, Istanbul, Türkiye
[5] Department of Earth Sciences, University of Sargodha, Sargodha, Punjab, Pakistan

* **Correspondence:** Email: ybashir@itu.edu.tr; dryasir.bashir@live.com; Tel: +90 5366 224 503.

Abstract: Seismic interpretation is primarily concerned with accurately characterizing underground geological structures & lithology and identifying hydrocarbon-containing rocks. The carbonates in the Netherlands have attracted considerable interest lately because of their potential as a petroleum or geothermal system. This is mainly because of the discovery of outstanding reservoir characteristics in the region. We employed global 3D seismic data and a novel Relative Geological Time (RGT) model using artificial intelligence (AI) to delve deeper into the analysis of the basin and petroleum resource reservoir. Several surface horizons were interpreted, each with a minimum spatial and temporal patch size, to obtain a comprehensive understanding of the subsurface. The horizons were combined with seismic attributes such as Root mean square (RMS) amplitude, spectral decomposition, and RGB Blending, enhancing the identification of the geological features in the field. The hydrocarbon potential of these sediments was mainly affected by the presence of a karst-related reservoir and migration pathways originating from a source rock of satisfactory quality. Our results demonstrated the importance of investigations on hydrocarbon potential and the development of 3D models. These findings enhance our understanding of the subsurface and oil systems in the area.

Keywords: artificial intelligence (AI); seismic interpretation; attributes; prospect; hydrocarbon

Abbreviations: %: Percentage; A: Amplitude; e(t): Instantaneous Amplitude; ft: Feet; *i*: *Imaginary section*; m: meter; m/sec: Meter per second; ms: millisecond; N: Number of Samples; Q: Quality Factor; R: Reflectivity; S: Seismic Trace; Sq: Square; *V*: Velocity m/sec;W: Wavelet; Z: depth; Zp: Acoustic Impedance; ω(t): Instantaneous Frequency; ρ: Density in g/cm^3; 3D: 3 Dimensional; AI: artificial intelligence; DFT: Discrete Fourier transform; DHI: Direct Hydrocarbon Indicator; H1: Horizon 1; HC: Hydrocarbon; Hz: Hertz; QC: Quality Control; RGT: Relative Geological Model; RMS: Root Mean Square; TDX: Total Horizontal Derivative; TVDss: True Vertical Depth SS.

1. Introduction

The North Sea is a continental shelf sea between Great Britain, the European continent, and the Scandinavian Peninsula. The North Sea connects with the Atlantic Ocean via the English Channel in the south and with the Norwegian Sea in the north. The North Sea is split up into several areas: Relatively shallow southern North Sea (including, e.g., the Southern Bight and the German Bight), the central North Sea, the northern North Sea, the Norwegian Trench, and the Skagerrak. It covers an area of 570,000 square kilometers, is more than 970 kilometers long, and is 580 kilometers wide [1]. The North Sea continental shelf is more than 1000 km long, and the water volume is estimated at 54,000 km³. The average depth of the North Sea is 94 m and increases around 200 m at the edge of the continental shelf toward the Atlantic Ocean. Based on [2], the sedimentary layers on the shelf are increasing northward towards the Arctic, reaching the highest values (12779.642 m) in the SW coast of Norway [2]. Ospar (2000) also stated that the Norwegian Trench, which features a sill depth of 270 m off the West Coast of Norway and a maximum depth of 700 m within the Skagerrak, plays a serious role in steering large inflows of Atlantic water into the North Sea [3]. The Channel is relatively shallow, with the Strait of Dover having a depth of about 30 m that gradually deepens to about 100 m in the west. Sea levels increased after the last glaciation and remained relatively stable for the past 6,000 years with only slight changes. The hydrographic circulation, wave, and tidal regime have influenced the sediment dynamics and distribution pattern observed today. Sand and gravel deposits are primarily found in the shallower areas, while fine-grained muddy sediments gather in many of the depressions [4].

Researchers have utilized seismic data, well logs, and a multi-layer feed-forward neural network (MLFN) to predict the link between porosity and impedance for reservoir characterization in the offshore F3 block of the Netherlands [5]. We utilized model-based seismic inversion (MBI) to estimate subsurface AI and then applied the MLFN algorithm to predict porosity in the inter-well region [6]. Based on the MBI result, the region contains loose rocks and no notable abnormal zone. Subsequently, the MLFN's prediction indicated a relatively high porosity, confirming the presence of a less compact formation in the area. It was determined that there is no substantial reservoir in the area. In a study by Sanda et al. (2020), seismic attributes were utilized to develop a method for characterizing the lithology of reservoirs. The data utilized for this study consisted of the 3D seismic data from block F3 in the Netherlands. We began by identifying the hydrocarbon zones using attributes like instantaneous amplitude energy, quality factor, and instantaneous frequency [7]. Detecting hydrocarbon zones involves identifying bright spots using attributes like instantaneous amplitude, energy, and Q-factor [8].

Next, the traps are localized by analyzing attributes like curvature, coherence, dip, and similarity to establish the reservoir boundaries. Identifying traps involves considering attributes such as curvature, similarity, dip, and coherence. At last, the seismic facies analysis involves choosing attributes like acoustic impedance, lambda, mhu, and the Vp/Vs ratio [9–12]. Moreover, by analyzing the combination of attributes and cross-plotting of data, we can enhance the lithological study of the reservoirs. In 2019, Kushwaha and colleagues applied the post-stack seismic inversion technique known as the Maximum Likelihood Sparse Spike inversion on 3D offshore seismic data from the F-3 Block in the Netherlands. This method is utilized due to its ability to generate high-resolution images of the subsurface, significantly improving seismic data interpretation [9]. One of the steps involved utilizing maximum likelihood deconvolution (MLD) to calculate the earth's reflectivity series, which was later transformed into impedance. The results suggest that the impedance and the variation of P-wave velocity were relatively low, indicating that the area has less compact rock. One of the categories that can be computed and extracted is geometrical attributes. These include similarity, fracture density, FEF on similarity, polar dip, maximum curvature, and thinned fault likelihood (TFL) attributes [14–17]. Additionally, the analysis of the inverted section revealed an abnormal zone possibly attributed to the reservoir zone's presence.

In 2018, Ishak, M.A et al. carried out a study demonstrating the significance of combining geological information, seismic attributes, sequence stratigraphic interpretation, and Wheeler transformation methods in recognizing geomorphological changes of stratigraphic surfaces [18]. In recent studies, advanced artificial intelligence tools have enhanced the subsurface potential [19,20]. These tools include seismic improvement and inversion techniques, wave modeling, machine learning, and various approaches to enhance the data [21–23]. The researchers utilized top-notch raw 3D seismic data obtained from block F3 in the North Sea Offshore of Netherlands [24]. The results revealed three depositional sequences, each consisting of packages including TST, HST, FSST, and LST, along with their corresponding stratigraphic surface. Observing the accumulation of sediment and changes in geomorphology on each stratigraphic surface is achieved by applying the appropriate seismic attribute. Hence, it is evident that combining geological data can effectively enable analysis of the basin's depositional environment and identifications of seismic and sub-seismic geomorphologic features.

1.1. F3 block offshore geology structure

The F3 block is on the shelf of the Dutch sector of the North Sea, as shown in Figure 1. The block is covered by 3D seismic that was acquired to explore for oil and gas in the Upper-Jurassic—Lower Cretaceous strata, which are found below the interval selected for this project. The upper 1200ms of the data set consists of reflectors belonging to the Miocene, Pliocene, and Pleistocene. The North Sea's core structural framework is mostly the consequence of extensional tectonics caused by failed rifting during the Late Jurassic and Early Cretaceous, and it is critical to understanding oil and gas traps in the North Sea [25,26]. According to these occurrences, the geological environment is split into three sections in relation to the major rifting episode. The first episode is distinguished by events and processes that occurred before the rifting (pre-rift). Syn-rift refers to the events and processes that occurred during the rifting event. Last, post-rift refers to the depositional processes and structural events that occurred after the Late Jurassic/Early Cretaceous [27].

Among the shelves of the North Sea Group, ten distinct geological units have been identified. The formations are listed from the oldest to the youngest: Limburg Group, Upper and Lower Rotliegend

groups, Zechstein Group, Lower and Upper Germanic Trias groups, Altena Group, Schieland, Scruff and Niedersachsen groups, Rijnland Group, Chalk Group, Lower and Middle North Sea groups, and Upper North Sea Group [28]. The significant sigmoidal bedding is noticeable, comprising deposits from a vast fluviodeltaic system that drained a large part of the Baltic Sea region [29,30]. The deltaic package comprises sand and shale, with a generally high porosity ranging from 20–33 percent. There are multiple streaks cemented with carbonate, and this package offers a range of fascinating features. One of the most prominent features is the extensive sigmoidal bedding, showcasing textbook-worthy downlap, toplap, onlap, and truncation structures. One can also observe bright spots, which are created by biogenic gas pockets. These are frequently found in this region of the North Sea. Identifying various seismic facies is crucial, including translucent, chaotic, linear, and shingles. Based on the well logs, the translucent facies display a consistently uniform lithology, potentially sand or shale. The disordered facies are probably a result of slumping deposits. The shingles at the base of the clinoforms consist of sandy turbidites.

The Netherlands is renowned for its natural gas production, mainly sourced from Carboniferous coal formations. The sandstones in the Lower Permian Rotliegend Formation make for exceptional reservoirs, sealed by the Upper Permian Zechstein carbonate and salt formations.

Comprising the Lower North Sea Group (Paleogene), Middle North Sea Group (Paleogene), and Upper North Sea Group (Neogene), the North Sea Group consists of three sub-formations. The Lower North Sea Group consists mostly of gray sands, sandstones, and clays, which were deposited in a marine environment at the periphery of the North Sea Basin due to multiple clastic sedimentation cycles of different sizes. At the top of the Chalk Group, there is a distinct lithologic break that acts as the lower boundary, with younger deposits of the Middle North Sea Group or other units above it unconformably. The Middle North Sea Group comprises various formations made up of sands, silts, and clays. The primary sand distribution occurs along the southern edge of the North Sea Basin. The group's depositional environment is believed to be mainly marine, with some lagoon and coastal plain sediments. Experts believe that the Upper North Sea Group consists of clays and sands ranging from fine-grained to coarse-grained, along with gravel, peat, and brown coal seams. There is a noticeable shift from coarse- to fine-grained sands in the northern and western areas of the North Sea Basin. The Middle North Sea Group and other older beds mark the lower boundary of this sub-group, with the current land surface or seafloor above serving as the upper boundary. The overall depositional environment is believed to be shallow marine settings and terrestrial beds of a fluvial and lacustrine origin. The highest section of this group might consist of glacial deposits.

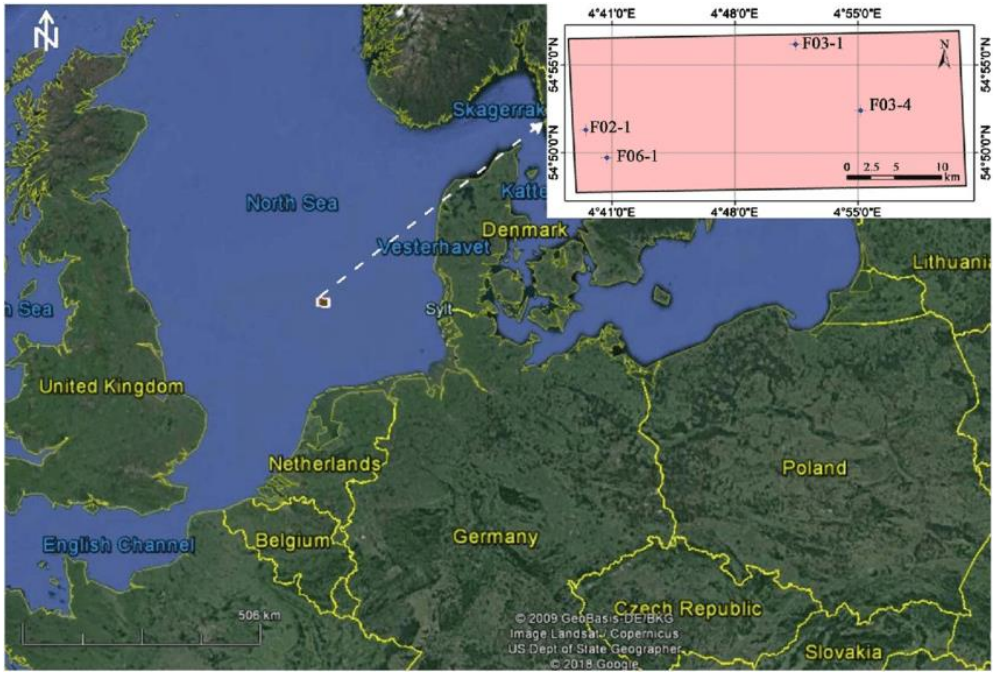

Figure 1. The F3-Block's location in the North Sea (Dutch sector) along with its wells (F02-1, F03-1, F03-4, and F06-1) displayed on Google Earth.

ERA	AGE		UNIT	THICKNESS (m)	LITHOLOGY	DESCRIPTION	DEPOSITIONAL SETTING
CENOZOIC	Quaternary / Neogene		Upper North Sea Group	1250 - 1290		Clays, fine to coarse grained sands, local gravels, coal seams	Shallow marine
	Paleogene	Oligocene	Middle North Sea Group	110 - 170		Clays, silts, and sands	Predominantly marine
		Paleocene - Eocene	Lower North Sea Group	220 - 500		Alternation of clays, marls, and sandstones	Predominantly marine
MESOZOIC	Cretaceous	Late	Chalk Group	30 - 420		Fine-grained limestones, and marly limestones. Local marls, calcerous claystones, glauconitic sands	Marine environment
		Early	Rijnland Group	50 - 60		Argillacious and some marly formations, sandstone beds, coarse clastic intercalations	Coastal, shallow to fairly deep open marine environment
	Jurassic	Late	Scruff Group	400 - 760		Local bituminous claystones, thin intercalated carbonate beds, and glauconitic, fine to coarse-grained sandstones	Marine environments from restricted (lagoonal) to open marine (outer shelf) conditions
			Schieland Group	360 - 1900		Claystones, coaly to clayey sandstones, rare coal seams, and local calcerous intercalations	Shallow marine to continental
	Triassic	Middle - Late	Upper Germanic Trias Group	60 - 100		Silty claystones, evaporites, carbonates, and sandstones	A series of sediments deposited in alternating shallow, restricted marine, and floodplain settings
PALEOZOIC	Permian	Late	Zechstein Group	> 220		Sequence of evaporites and carbonates with some thin intercalations of claystone	Peri-marine to marine setting

Figure 2. Generalized lithologic column of the survey area [29].

In summary, the North Sea Group comprises geological formations that originated in the Tertiary and Quaternary periods. The formation is segmented into three sub-categories: The Lower North Sea Group, Middle North Sea Group, and Upper North Sea Group [30]. Every subgroup exhibits distinct lithology and depositional settings.

1.2. Tectonic framework and stratigraphy

The Eridanos delta system, also referred to as the fluvial-deltaic system of the North Sea Basin, began to form in the Oligocene and continued to develop throughout the late Cenozoic Period. In the Oligocene era, the Fennoscandian shield began to uplift, while the North Sea Basin underwent subsidence. Many researchers have theorized that the Fennoscandian shield experienced rapid uplift during the late Miocene. At this time, due to the accelerated rate of uplift, the Netherlands North Sea region experienced a significant influx of sedimentation. This event has caused the underlying Permian Zechstein salt to start shifting because of variations in load across the region. Localized unconformities have developed as a result of the migration of the underlying Permian Zechstein, leading to the formation of salt domes. There are different levels of Cenozoic succession shown in Figure 2. The upper packages consist of coarse-grained Neogene sediment, while the lower packages consist of fine-grained gradational Paleogene sediments [18,28,30–33]. The North Sea Basin, a region with diverse geology, displays a stratigraphy that has been influenced by millions of years of sedimentation and tectonic activity. The basin's layers of sediment showcase a range of ages, from Paleozoic to Holocene, revealing different geological events and environmental conditions. The basin began to take shape in the late Paleozoic era due to the splitting of the supercontinent Pangaea, resulting in the accumulation of thick layers of Triassic, Jurassic, and Cretaceous sediments. Later geological shifts, such as compression during the Alpine mountain-building event, continued to impact the formation and layers of sediment in the basin. The North Sea Basin evolved during the Cenozoic era, experiencing substantial deposition in the Paleogene and Neogene periods, leading to the creation of abundant hydrocarbon reservoirs. The Pleistocene era was characterized by glacial and interglacial cycles that influenced erosional and depositional processes. In contrast, the Holocene era introduced modern sedimentation patterns influenced by sea-level fluctuations and human activities. Overall, the stratigraphy of the North Sea Basin offers a valuable account of geological history, which is crucial for grasping its hydrocarbon potential and environmental dynamics. This basin consists of nine units of stratigraphic groups that lasted from the Palaeozoic era to the Cenozoic [29].

1) Zechstein Group (Palaeozoic). This group was formed in the Late Permian period. This group consists of a series of evaporites and carbonates with some thin intercalations of claystone. The depositional environment ranges from peri-marine to marine.

2) Upper Germanic Trias Group (Mesozoic). This subgroup was formed during the middle to late Triassic period. This group consists of silty claystone, anhydrous evaporites carbonates, and sandstones. This group setting involves a sequence of sediments that were deposited in alternating shallow restricted marine and floodplain environments.

3) Scruff Group (Mesozoic). This group was formed in the Late Jurassic period and was deposited in the Late Jurassic period. The Scruff Group consists of local bituminous claystone, thin intercalated carbonate layers, and glauconitic sandstones of fine and coarse grains. They possess oceanic habitats ranging from the lagoon to outer shelf conditions.

4) Schieland Group (Mesozoic). The Schieland Group consisted of claystone, coal, clayey

sandstones, occasional coal seams, and calcareous intercalations. The environment ranges from shallow sea to continental.

5) Chalk Group (Mesozoic). The Chalk Group was formed in the Late Cretaceous period. The Chalk group is composed of fine-grained limestones, marly limestones, local marls, calcareous claystone, and glauconitic sands. This group consists of marine settings.

6) The Rijnland Group (Mesozoic). This group was deposited in the Early Cretaceous period. The composition includes argillaceous and marly strata, sandstone beds, and coarse clastic intercalations. The area also includes coastal regions and a variety of marine ecosystems ranging from shallow to deep open waters.

7) Lower North Sea Group (Cenozoic). This group was deposited during the Paleogene period, namely the Paleocene-Eocene epoch. The composition consists of alternating layers of clays, marls, and sandstones. The setting is primarily marine.

8) The Middle North Sea Group was deposited during the Paleogene period, specifically in the Oligocene epoch of the Cenozoic era. The composition primarily consists of clays, silts, and sands. The setting is mostly focused on the sea.

9) Upper North Sea Group refers to a geological formation from the Cenozoic era. Deposited during the Neogene era, this formation consists of clays, fine and coarse-grained sands, local gravels, and coal seams. The environment is a shallow marine setting.

2. Database, workflow, and methods

2.1. Subsurface data

The 3D post-stack time-migrated seismic grid data is from the F3-block, covering approximately 386.92 sq km area, acquired from dGB Earth Sciences via its open-source seismic repository portal. The seismic data was sampled at 4 ms intervals, the dominant frequency of the data is 40 Hz with a total duration of approximately 1.8 s, and a bin size of 25 m. No conditioning was applied to the data as it was provided in a stacked and migrated format. Dealing with initial conditioning involved addressing various sources of noise, correcting seismic velocities that may have been over or under-corrected, dealing with frequency distortions, and mitigating other undesirable effects that were already applied to the provided data. In addition to the 3D seismic data, two seismic lines were analyzed. Figure 3 shows the inline 462.

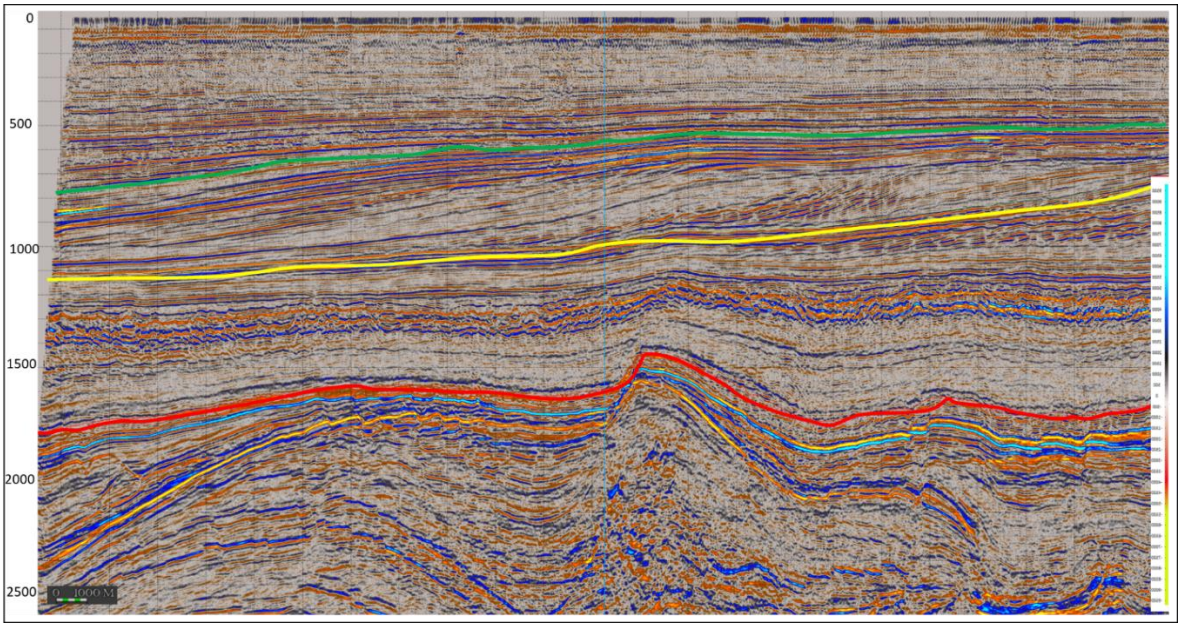

Figure 3. Inline 462 with three chosen horizons have been interpreted (Green: H83, Yellow: H59 and Red: H15).

Understanding seismic data is crucial in the oil and gas sector, playing a key role in exploration and production activities. Precisely defining the subsurface geology is essential for effectively exploiting known hydrocarbon accumulations. However, seismic interpretation can be a challenging and lengthy process since manual seismic data labeling can require weeks, months, or years. Moreover, due to the extensive dataset it entails, advanced software like PaleoScan can significantly decrease the interpretation time cycle and quickly improve geological understanding. We utilized an advanced seismic method developed by Pauget et al. to generate a 3D Relative Geological Time (RGT) model from the 3D seismic volume [33]. Using a 3D RGT model, seismic attributes were also utilized to emphasize geological characteristics and aid in the structural imaging and interpretation of the F3 North Sea, Netherlands' seismic volume. We offer a modest addition to the seismic interpretation of The Netherlands interpretation dataset. The dataset from the Netherlands F3 covers a seismic survey area of 386.92 sq km in the Dutch offshore section of the Central Graben basin, located about 180 km off the Dutch shore. The coordinates are N 54° 52' 0.86"/E 4° 48' 47.07".

2.2. Seismic attributes

Seismic attributes are quantities derived from seismic data, which can be studied to enhance subtle information in a traditional seismic image for improved data interpretation. Seismic attributes are commonly utilized by geologists and geophysicists for interpreting seismic data. This method is effective in numerous studies for various objectives [34,35]. All seismic features result from a linear combination of these three fundamental variables. It is essential to consider all information from these attributes when analyzing seismic data, including amplitude, phase, and frequency [36,37]. Figure 4 illustrates how these parameters combine to determine the specific attribute for seismic interpretation.

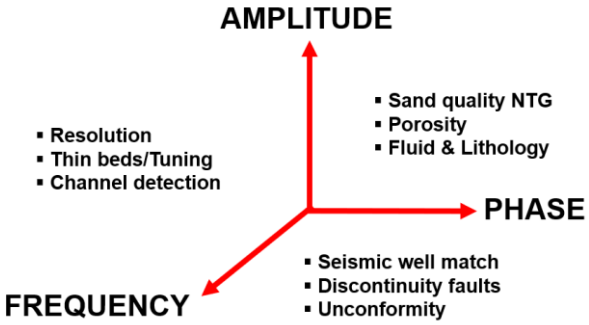

Figure 4. Seismic variables and their attributes are best represented in a triangular shape with respect to their connection to one another.

Amplitude: This indicates the strength or intensity of seismic reflections captured at every location in the subsurface. The variations are a result of differences in the rock properties like lithology, porosity, and fluid content. Increased amplitude reflections usually suggest boundaries between different geological formations, like a sandstone reservoir on top of a shale caprock. Utilizing amplitude attributes is essential for outlining geological characteristics, pinpointing potential hydrocarbon reservoirs, and visualizing structural and stratigraphic differences.

Phase: The phase indicates the timing relationship between seismic waveforms at various receivers. This content discusses the timing of seismic reflections, which may vary due to changes in rock properties, structural complexity, and seismic wave propagation. Phase attributes are essential for outlining geological features, identifying faults, and describing stratigraphic variations. For instance, a change in phase across a fault plane may suggest fault displacement.

Frequency: The frequency indicates how often seismic waves oscillate and is linked to the level of detail in subsurface imaging. High-frequency seismic waves offer a more detailed view, enabling the identification of thin beds, small-scale faults, and subtle stratigraphic features. Waves with lower frequencies can reach greater depths underground but provide less detailed images. Frequency attributes play a crucial role in reservoir characterization, lithology discrimination, and identifying sedimentary facies variations.

When analyzing seismic data, these characteristics are frequently examined collectively to develop a thorough comprehension of underground geology. For instance, differences in amplitude may correspond with variations in lithology recognized through phase information. Identifying reservoir sweet spots is facilitated by analyzing frequency attributes that consider variations in porosity and permeability. By combining various seismic attributes, geological interpretation can be enhanced, leading to better identification of potential exploration targets or strategies for reservoir management. In this research, 3 seismic attributes have been incorporated to image the geological features of the F3 block of the North Sea, the further details of attributes are as below.

2.2.1. RMS amplitude, spectral decomposition, and color blending

The root mean square amplitude (RMS amplitude) is a commonly used technique to display amplitude values in a specified window of stack data. These attributes are widely used in the identification of bright spots, zones of hydrocarbons, channels, and other geological features. In

seismic data, sometimes reflections from the top and bottom layers create a constructive interference known as a thin-bed stunning effect. As a result, some of the layer thickness will not appear in the seismic section. In spectral decomposition, the seismic data is converted from the time domain or depth to the frequency domain. Each individual frequency response gave different information on geological features. Spectral decomposition decomposes the seismic data with normal frequency bandwidth into a set of sections having discrete or very narrow bandwidth (Figure 5). It is based on the concept that reflections from a thin bed have a characteristic expression in a particular frequency domain that is indicative of temporal bed thickness. It is also very effective in mapping stratigraphic features such as Channels. By combining three frequency responses using RGB blends, the interplay between different frequency responses becomes more apparent [38–41]. As a result, a high resolution of blended frequency images can be obtained where the geological features are highlighted more clearly.

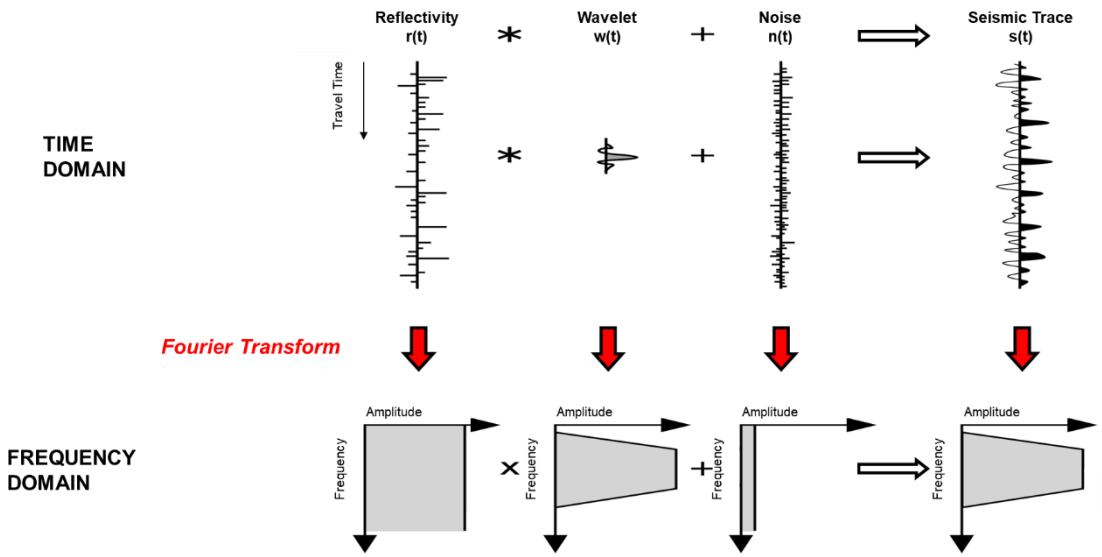

Figure 5. the process of Time Vs Frequency Domain Convolution with respect to a diverse amplitude spectrum.

It is well-established that a convolution in the time domain is equivalent to a multiplication in the frequency domain. When multiplying two frequency signals in polar form, you multiply their magnitude components and add their phase components.

Time-domain convolution and frequency-domain convolution are algorithms employed in the processing of signals and are closely connected through the convolution theorem. When working with signals in the time domain, convolution is the process of combining two signals by multiplying them together and then integrating the result over time. This allows us to express the output signal as a combination of shifted and scaled versions of the input signals. On the other hand, frequency-domain convolution involves the utilization of Fourier transforms to process the input signals. This is achieved by multiplying the transformed signals in the frequency domain and subsequently converting the outcome back to the time domain using the inverse Fourier transform. Computing convolution in the frequency domain offers computational advantages, particularly for linear time-invariant systems, as it simplifies the process into a pointwise multiplication. This transformation is widely used in various applications, including audio processing, image processing, and communication systems. It helps to

improve filtering, modulation, and signal analysis, making these processes more efficient. Deciding whether to use time or frequency domain convolution relies on the unique properties of the signals and the computational needs of the application at hand.

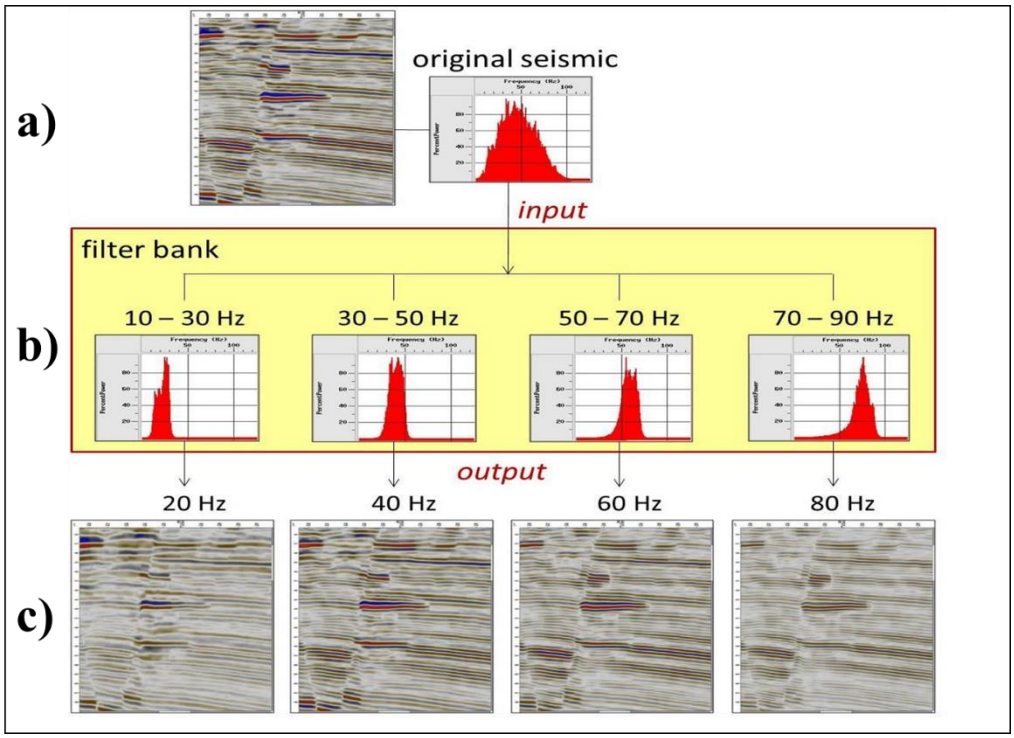

Figure 6. Graphical representation of narrowband filters. a) The input data and frequency spectrum, b) filter bank of data based on frequency range, and c) convert filtered output to reflection strength to obtain frequency measures of seismic data.

Spectral decomposition in the context of seismic data analysis is mainly focused on filtering, as demonstrated in Figure 6. The process involves analyzing a seismic signal (Figure 6b) and separating it into its individual frequency components (Figure 6c). This process is accomplished using various mathematical techniques, including the Fourier transform. Through the process of decomposing seismic data into various frequency bands, geoscientists can amplify particular geological characteristics and detect irregularities linked to hydrocarbons or other underground structures. Simply put, spectral decomposition functions as a specialized filter that focuses on specific frequency ranges, enabling a more comprehensive and understandable examination of seismic data in the study and description of underground reservoirs in the oil and gas sector.

2.2.2. Physical Factors Affecting Seismic Attributes

Various physical factors in the subsurface affect seismic attributes. Thus, understanding the characteristics of rocks is essential, encompassing elements like lithology, porosity, density, and elastic moduli. The properties listed in Table 1 are essential for determining the speed and attenuation of seismic waves. These factors greatly influence the characteristics of seismic reflections. Furthermore, the dynamic nature of the content is crucial, as alterations in the distribution of water, oil, or gas can

affect the acoustic characteristics of rocks beneath the surface. Hydrocarbons, for example, can result in distinct seismic signatures. Furthermore, the structure of rocks, specifically through faulting and folding, has a significant impact on seismic attributes as it alters the path of seismic waves. Understanding these physical factors is essential for accurately interpreting seismic data and gaining insights into the underlying geology. This knowledge is highly valuable in applications such as hydrocarbon exploration and reservoir characterization. There are multiple factors that affect the seismic attribute, which are summarized based on our research in Table 1.

Table 1. The list for physical factors that affect the seismic attributes.

Amplitude	Frequency	Phase
Wavefield Divergence	Source Bandwidth	Source and recording filter
Absorption-Dispersion	Ghost, Absorption & Scattering	Ghosting
Transmission	Source and hydrophone	Absorption
Pegleg Multiples	development depth	De-signature
Thin bed Tuning	Source volume and depth	-

In traditional seismic interpretation, the focus is primarily on a few horizons that are selected either manually or through auto-tracking. The current workflow can be quite time-consuming and often requires geoscientists to make numerous assumptions, especially when dealing with low signal quality or complex geology. The Model is designed to minimize the cost function, which is influenced by the following factors: Comparing seismic data for similarity and calculating the distance between seismic points.

The ideal model is associated with the lowest cost. To achieve the most precise geological outcomes, it is possible to incorporate geological limitations such as faults and horizons into the optimization procedure.

3. Results and discussion

Creating a Relative Geological Time model (RGT) straight from the seismic is an innovation in the interpretation workflow. There are two steps to creating an RGT model using this method. First, a seismic volume is selected for computing a geological Model Grid. By a cost function minimization algorithm, a number of nodes are distributed in the seismic volume. Then, each node is linked according to the similarity of the wavelets and relative distance. Via this advanced algorithm, all potential horizons within the seismic volume are auto-tracked, and a Relative Geological Time is computed for all horizons without overlaps with each other. Second, the Relative Geological Time Model is generated from the Model Grid, and each sample of the seismic volume is now assigned with relative geologic time.

From the RGT Model, a horizon stack corresponding to the relative ages of the Model can be derived into horizons. Multiple attributes, such as Spectral decomposition, RMS Amplitude, and Color-blended Spectral Decomposition, can be applied to these horizons. In this work, 100 horizons are picked between the top and base. These horizons are then evaluated and examined to find the observable expression. This Horizon Stack allows better strata slicing via the seismic volume, as most expressions can be highlighted.

For interpreting seismic data, we have chosen 4 horizon and surface maps to show the effectiveness of attributes and enhanced interpretation. Comparing various attributes like Spectral decomposition (Figure 7a), RMS amplitude (Figure 7b), and RGB blending (Figure 7c) helps highlight the bright spot that certain applications struggle to detect. This bright spot can sometimes get mixed with the reflection amplitude. Examining the surface map in Figure 8a-c provides a detailed insight into the bright spot phenomenon. RMS amplitude is utilized to analyze this geological feature due to its varying parameters like velocity and density. The seismic reflection data can be affected during acquisition, and a higher acoustic impedance contrast may result in a higher amplitude, leading to better illumination of the bright spot in the subsurface, as demonstrated in Figures 7 and 8. From the RMS Amplitude seismic attribute in Figure 8b, there are 2 distinct features of geological expression: Pockmark and hydrocarbon prospecting zone. These two features are indicated by the bright spots. Pockmark is a common feature that can be found in the seabed of the North Sea region due to biogenic gas and liquid escaping or a dewatering event which is ordinary in this region [41].

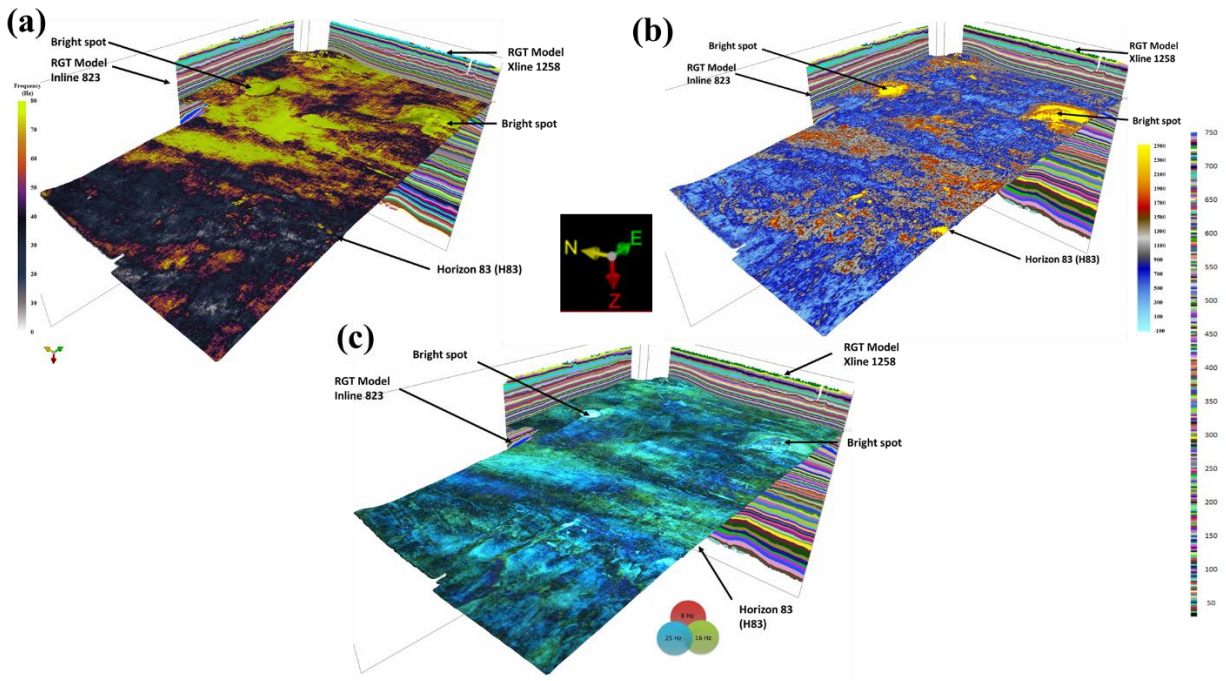

Figure 7. Seismic attributes application for visibility enhancement of subsurface features. a) Spectral decomposition, b) RMS Amplitude, and c) RGB Blends (Color-blended method).

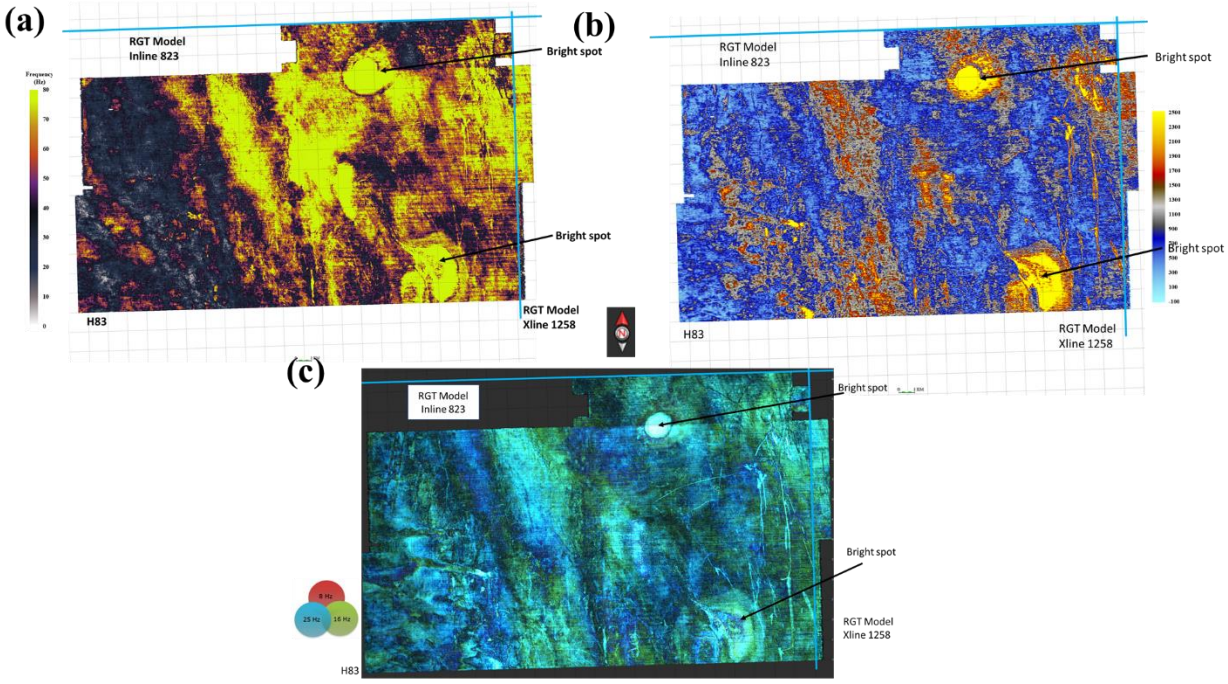

Figure 8. Top view of the surface map of Horizon 83. a) Spectral decomposition, b) amplitude, and c) RGB Blends (Colour-blended method).

Other than the amplitude, RGB, and spectral decomposition there are three frequencies that have been defined as low frequency (30 Hz), middle frequency (46 Hz), and high frequency (65 Hz), as shown in Figure 9a-c, respectively. These three frequencies are used as the input for the Horizon Stack Color-Blended. Then, the single output images, RGB Horizon Stack Color-Blended, are produced (Figure 9 in surface and Figure 10 as a time slice of the horizon).

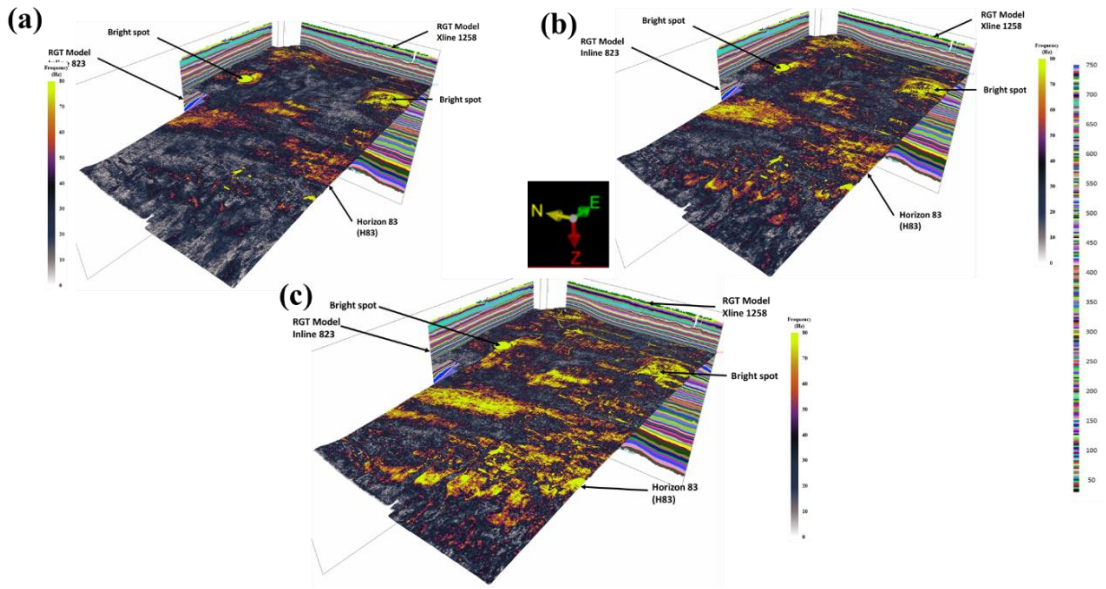

Figure 9. RGT model of inline 823 and xline 1258 with surface horizon attribute spectral decomposition. a) 30 Hz, b) 46 Hz, and c) 65 Hz.

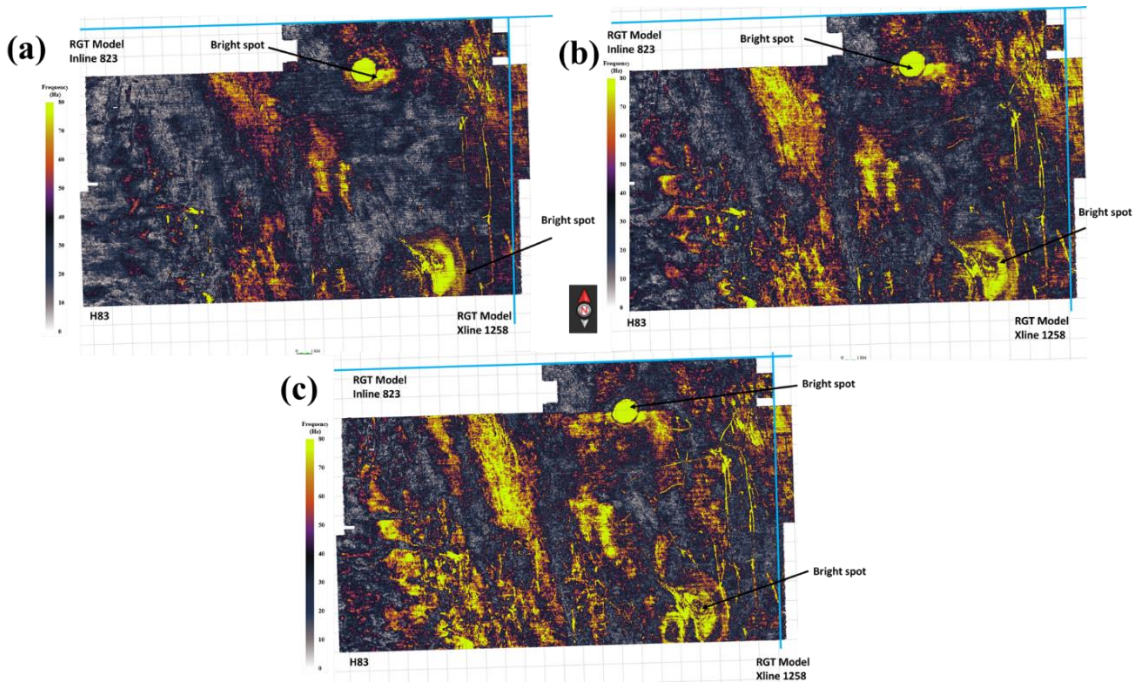

Figure 10. H83 with spectral decomposition attribute application. a) 30 Hz, b) 46 Hz, and c) 65 Hz. Comparison between the three frequencies. The 46 Hz of Spectral Decomposition gives a better resolution of the channel features (red, oval shape). This could be because 46 frequency is the tuning frequency where the channel's geometry is pronounced.

Furthermore, in Figure 11, two channel-like features can be observed on horizon 59, as shown in the multi-attribute representation using Spectral decomposition (Figure 11a), RMS amplitude (Figure 11b), and RGB Blending (Figure 11c). The RMS and RGB Blend section provides a more distinct illustration of these channels in contrast to the Spectral decomposition attribute, helping us comprehend and acquire valuable insights into the different ways the attribute applications are utilized.

Additional fault detection applications for multiple seismic attributes have been utilized to identify a fault at horizon H59. The analysis indicates a combination of channel and fault, which appear similar in the top view or horizon slice, as illustrated in Figure 12. Three attributes, including Spectral decomposition (Figure 12a), RMS amplitude (Figure 12b), and RGB blending (Figure 12c), were carefully examined in the top view of the surface, with the most accurate representation of the fault found in the RGB blending attribute. It effectively distinguishes the fault and channel with precision and insight.

Similarly, to the amplitude, RGB, and Spectral decomposition, three frequencies have been defined as low frequency (30 Hz), middle frequency (46 Hz), and high frequency (65 Hz) for horizon 59 to show the channel illumination in spectral decomposition, as shown in Figure 13a-c, respectively. These three frequencies are used as the input for the Horizon Stack Color-Blended. Then, the single output images, RGB Horizon Stack Color-Blended, are produced (Figure 13 in surface and Figure 14 as a time slice of the horizon).

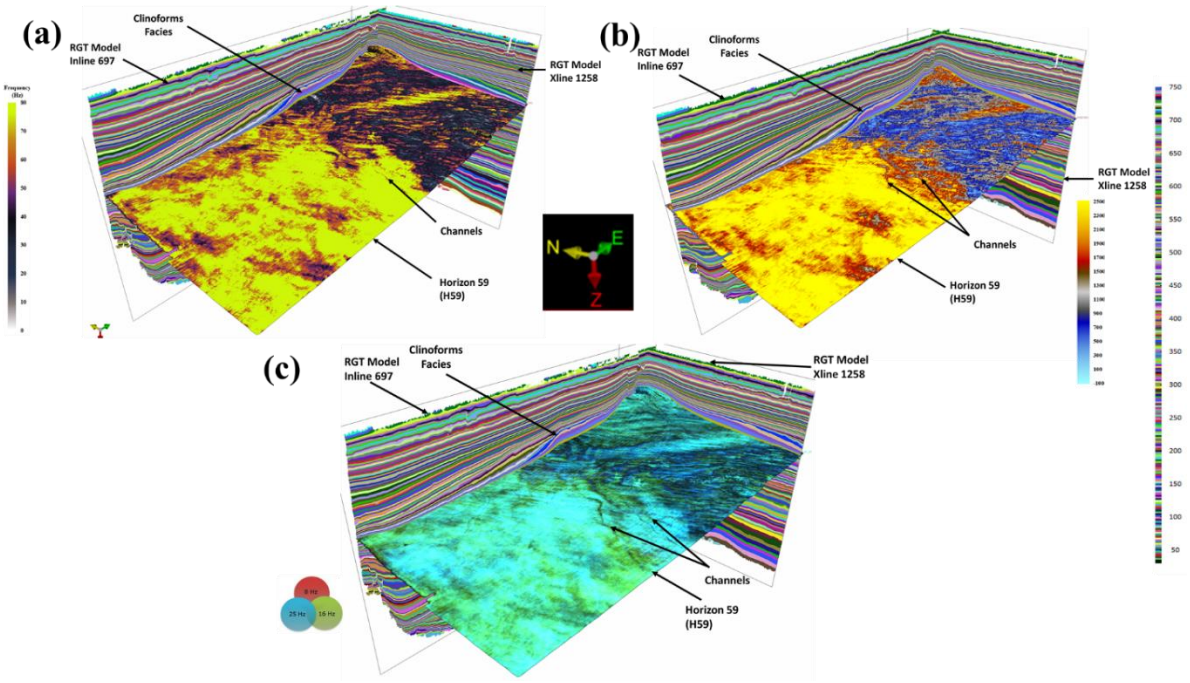

Figure 11. Seismic attributes application for visibility enhancement of subsurface features. a) Spectral decomposition, b) RMS Amplitude, and c) RGB Blends (Color-blended method).

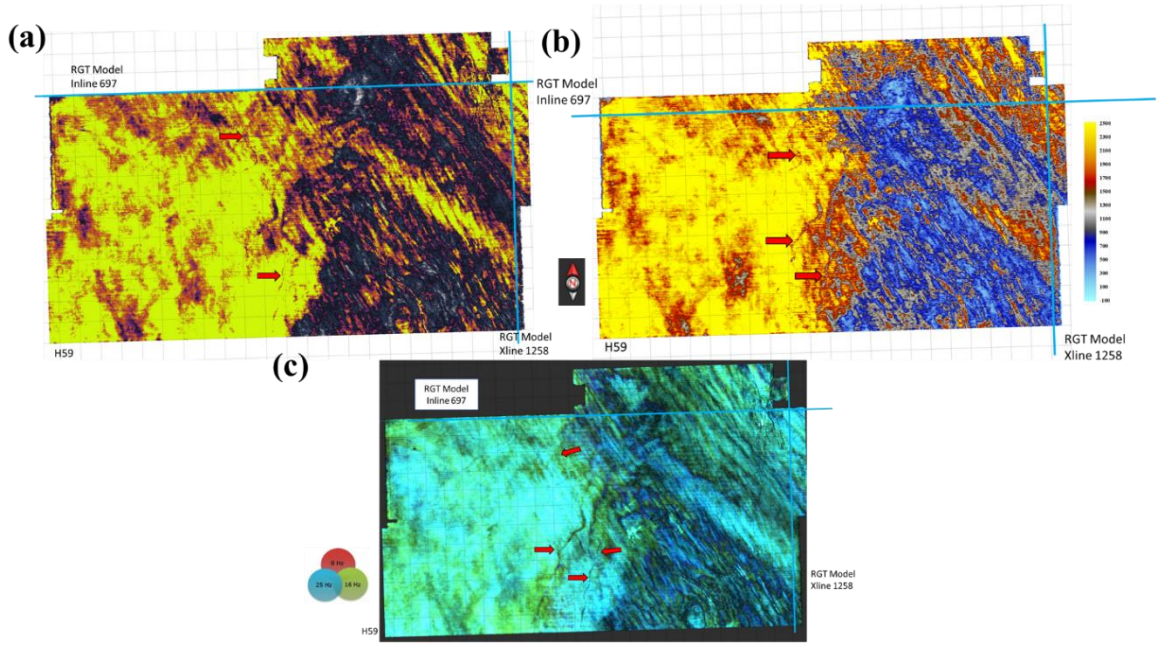

Figure 12. Discussing the geological characteristics of horizon H 59, including a) Spectral decomposition, b) Amplitude, and c) RGB Blended. The red arrow shows the continuity of the faults clearly in the RGB results.

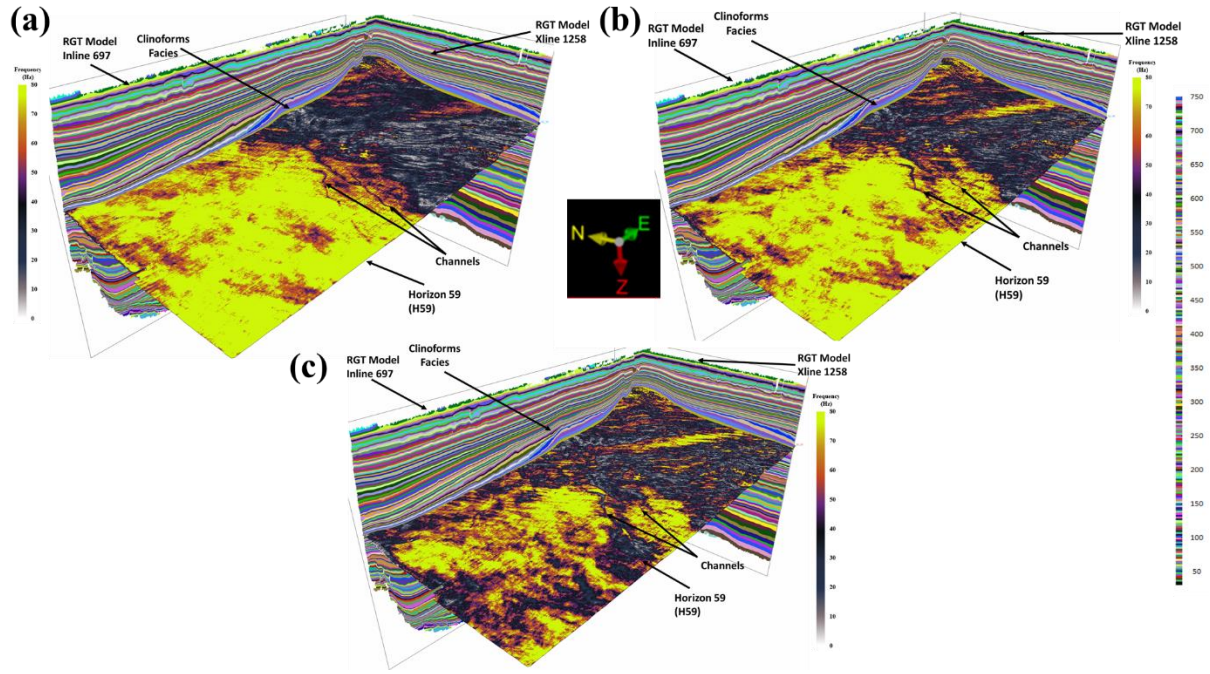

Figure 13. Surface maps of the H59 with spectral decomposition attribute application. a) 30 Hz, b) 46 Hz, and c) 65 Hz.

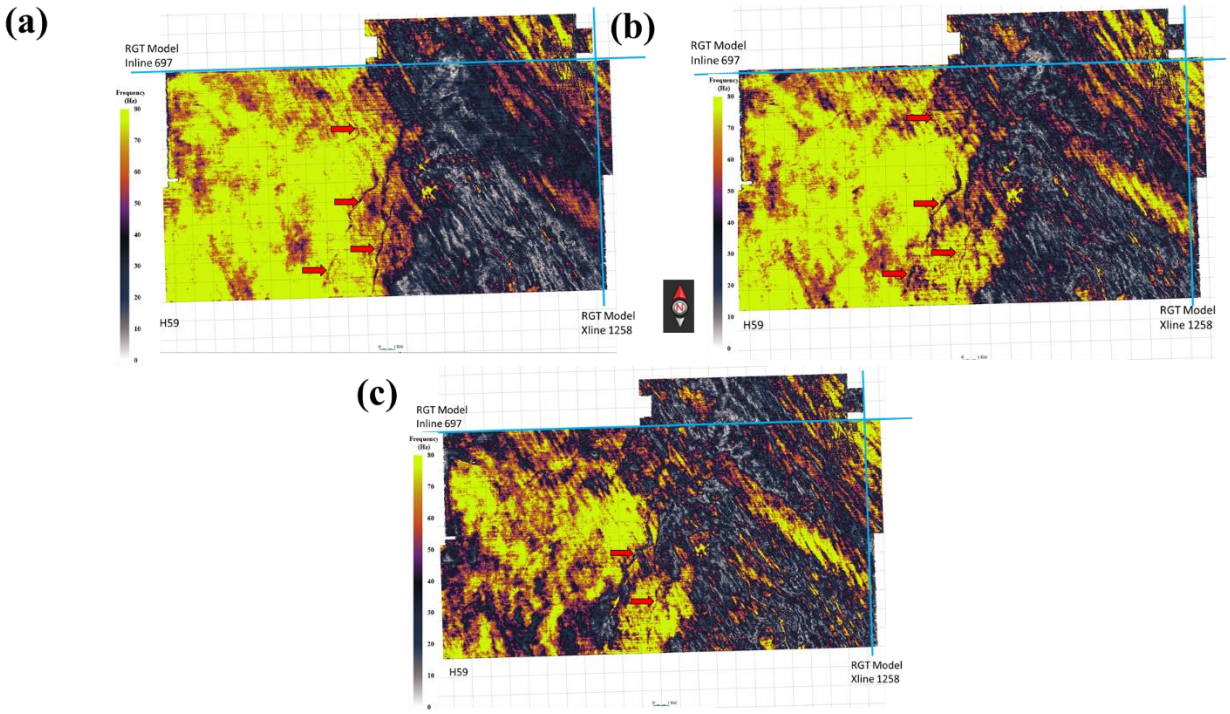

Figure 14. Top view of Horizon 59 with comparison of different frequencies. a) 30 Hz, b) 46 Hz, and c) 65 Hz. In this case, the lower frequency gives the better continuity of the fault, but the sediments are distributed.

Seismic interpretation can be a time-consuming task. Interpreting 2D seismic sections is a meticulous process that can span over several weeks or even months to analyze all the desired horizons. The algorithm used to develop the RGT model consisted of a specific patch size in the x and y directions. This approach greatly decreased the time needed for interpreting horizons without compromising accuracy.

Choosing the right seismic attributes is crucial for effectively executing the workflow outlined in this study. A summary of the application's output is presented in Table 2, providing insights to better understand the attributes and applications within the study area. For our application, the optimal attributes included seismic Spectral decomposition, RMS amplitude, RGB blending, and Spectral decomposition with diverse frequencies. Since the impedance is directly related to the elastic parameter of the formation, it would be beneficial to incorporate the impedance attribute into the automatic horizon tracking. Traditionally, the process of seismic attributes workflow can be quite time-consuming. On the other hand, the advanced application can extract many horizons with various seismic attributes from the Relative Geologic Time model. For example, Figures 7b, 8b, 11b, and 12b show RMS amplitude, while Figures 7a, 8a, 9, 10, 11a, 12a, 13, and 14 depict Spectral Decomposition. Additionally, Figures 7c, 8c, 11c, and 12c display RGB blending.

Two distinct geological features can be identified from the RMS Amplitude seismic attribute: A pockmark and a hydrocarbon prospecting zone. These two characteristics are highlighted by the bright spots. Pockmarks are a prevalent characteristic in the seabed of the North Sea region, often caused by the escape of biogenic gas and liquid or dewatering events that are typical in this area. Additionally, a channel-like feature is visible in horizon 59.

Table 2. A summary of geophysical attributes and the impact of their implementation in the research region.

Name of Seismic Attribute	Provides Basic Seismic Information	Type of Seismic Attribute	Outcome in the Study Area
RMS Amplitude	Energy of the seismic trace, Stratigraphic and reservoir	Complex trace attribute	RMS amplitude provides a clearer representation of channels and geological features.
RGB Blending (Color Blended method)	Frequency or amplitudes at three offsets and comprehensive interpretation	Complex trace attribute	RGB blends showcase the interaction between various frequency responses, which becomes more noticeable in the desired structure.
Spectral Decomposition	Frequency and provide Stratigraphic and reservoir.	Complex trace attribute	Time-varying spectral characteristics of seismic data is a valuable indicator of isolating lower frequency areas at the edges of the input data set, potentially highlighting bright spots.

Seismic attributes are essential for subsurface interpretation and oil & gas exploration as they offer quantitative measurements to characterize geological features and identify potential hydrocarbon reservoirs. Amplitude attributes aid in defining geological formations and identifying reservoirs by analyzing differences in rock properties. Phase attributes help identify structural features such as faults

and stratigraphic variations. Frequency attributes offer a comprehensive view of subsurface formations, assisting in reservoir analysis and distinguishing rock types. By incorporating these characteristics, exploration teams can improve their grasp of subsurface geology, pinpoint exploration targets, and refine reservoir development strategies, boosting the efficiency and success rate of oil and gas exploration and production activities.

4. Conclusions

We present the effectiveness of a technique called the "Global seismic interpretation method". This proposed cutting-edge method can convert 3D seismic data into a 3D RGT model. Moreover, this approach significantly reduces the time spent by interpreters for extracting hundreds of horizons from a 3D or 2D seismic dataset, which is achieved in a short amount of time. Afterward, the selected seismic attributes are applied to these horizons. Based on the findings, this approach has been extremely beneficial for interpreters in a wide range of applications, including subsurface imaging, stratigraphic imaging, structural, and quantitative interpretation, as well as exploration and reservoir characterization.

In future projects, additional seismic attributes might be utilized to reveal numerous concealed characteristics within the seismic volume. For example, curvature attributes are a powerful tool for interpreting and visualizing structural features. Identifying variance attributes can help in distinguishing geological features like deltas, faults, and karst. Furthermore, the channel's feature can be more clearly defined by combining Spectral decomposition attributes with the coherence attribute.

Author contributions

YB: Conceptualization, Methodology, Software, Formal analysis, Writing: Original Draft, Funding acquisition, MAAZ: Software, Formal analysis, Writing - Original Draft, Data Curation, AK: Supervision, Methodology, Writing: Review & Editing, Visualization, DD: Conceptualization, Writing: Review & Editing, Project administration, ZD: Writing: Review & Editing, Project administration, AM: Writing: Review & Editing, Project administration, SHA: Software, Formal analysis, Writing: Original Draft.

Acknowledgments

We want to express our sincere appreciation to the Geophysical Engineering Department at Istanbul Technical University in Turkey and the School of Physics, Geophysics section at Universiti Sains Malaysia for providing the facilities for this research. We thank dGB Earth Sciences for making the data available as an OpendTect project via their TerraNubis portal terranubis.com. This research was funded by Disiplinlerarası Araştırma Projesi (DAP) BAPSIS ITU Research project code TDA-2023-44996 and project ID-44996.

Ethics approval

All ethical standards have been followed during this research.

Data Availability

Data will be available on demand

Use of AI tools declaration

The authors declare they have not used Artificial Intelligence (AI) tools in the creation of this article.

Conflict of interest

The authors declare no competing interest.

References

1. Lemenkova P (2020) Integration of geospatial data for mapping variation of sediment thickness in the North Sea. *Sci Annals Danube Delta Inst* 25: 129–138. https://doi.org/10.7427/DDI.25.14
2. Polina L (2000) Integration of geospatial data for mapping variation of sediment thickness in the North Sea. Scientific Annals of the Danube Delta Institute. https://doi.org/10.7427/DDI.25.14
3. Quante M, Colijn F (2016) *North Sea region climate change assessment*, Springer Nature.
4. Kushwaha PK, Maurya SP, Singh NP, et al. (2019) Estimating subsurface petro-physical properties from raw and conditioned seismic reflection data: a comparative study. *J Indian Geophys Union* 23: 285–306.
5. Bashir Y, Siddiqui NA, Morib DL, et al. (2024) Cohesive approach for determining porosity and P-impedance in carbonate rocks using seismic attributes and inversion analysis. *J Petrol Explor Prod Technol* 14: 1173–1187. https://doi.org/10.1007/s13202-024-01767-x
6. Sanda O, Mabrouk D, Tabod TC, et al. (2020) The integrated approach to seismic attributes of lithological characterization of reservoirs: case of the F3 Block, North Sea-Dutch Sector. *Open J Earthquake Res* 9: 273–288. https://doi.org/10.4236/ojer.2020.93016
7. Hermana M, Ghosh DP, Sum CW (2017) Discriminating lithology and pore fill in hydrocarbon prediction from seismic elastic inversion using absorption attributes. *Leading Edge* 36: 902–909. https://doi.org/10.1190/tle36110902.1
8. Babasafari AA, Bashir Y, Ghosh DP, et al. (2020) A new approach to petroelastic modeling of carbonate rocks using an extended pore-space stiffness method, with application to a carbonate reservoir in Central Luconia, Sarawak, Malaysia. *Leading Edge* 39: 592a1–592a10. https://doi.org/10.1190/tle39080592a1.1
9. Bashir Y, Babasafari AA, Alashloo SYM, et al. (2021) Seismic wave propagation characteristics using conventional and advance modelling algorithm for d-data imaging. *J Seism Explor* 30: 21–44.
10. Bashir Y, Ghosh DP, Babasafari A (2019) Wave propagation characteristics using advance modelling algorithm for D-Data imaging. SEG International Exposition and Annual Meeting, San Antonio, Texas, USA, 3795–3799. https://doi.org/10.1190/segam2019-3215236.1
11. Shoukat N, Ali SH, Siddiqui NA, et al. (2023) Diagenesis and sequence stratigraphy of Miocene, Nyalau Formation, Sarawak, Malaysia: A case study for clastic reservoirs. *Kuwait J Sci* 50: 790–802. https://doi.org/10.1016/j.kjs.2023.04.003

12. Kushwaha PK, Maurya SP, Rai P, et al. (2020) Use of Maximum Likelihood Sparse Spike Inversion for Reservoir Characterization-A Case Study from F-3 Block, Netherland. *J Petrol Explor Prod Technol* 10: 829–845. https://doi.org/10.1007/s13202-019-00805-3
13. Ismail A, Radwan AA, Leila M, et al. (2023) Unsupervised machine learning and multi-seismic attributes for fault and fracture network interpretation in the Kerry Field, Taranaki Basin, New Zealand. *Geomech Geophys Geo-Energy Geo-Resour* 9: 122. https://doi.org/10.1007/s40948-023-00646-9
14. Ismail A, Ewida HF, Al-Ibiary MG, et al. (2021) The detection of deep seafloor pockmarks, gas chimneys, and associated features with seafloor seeps using seismic attributes in the West offshore Nile Delta, Egypt. *Explor Geophys* 52: 388–408. https://doi.org/10.1080/08123985.2020.1827229
15. Ismail A, Radwan AA, Leila M, et al. (2024) Integrating 3D subsurface imaging, seismic attributes, and wireline logging analyses: Implications for a high resolution detection of deep-rooted gas escape features, eastern offshore Nile Delta, Egypt. *J Afr Earth Sci* 213: 105230. https://doi.org/10.1016/j.jafrearsci.2024.105230
16. Azarafza M, Ghazifard A, Akgün H, et al. (2019) Development of a 2D and 3D computational algorithm for discontinuity structural geometry identification by artificial intelligence based on image processing techniques. *Bull Eng Geol Environ* 78: 3371–3383. https://doi.org/10.1007/s10064-018-1298-2
17. Misra S, Li H, He J (2019) *Machine learning for subsurface characterization*, Gulf Professional Publishing.
18. Zhang H, Chen T, Liu Y, et al. (2021) Automatic seismic facies interpretation using supervised deep learning. *Geophysics* 86: IM15–IM33. https://doi.org/10.1190/geo2019-0425.1
19. AlRegib G, Deriche M, Long Z, et al. (2018) Subsurface structure analysis using computational interpretation and learning: A visual signal processing perspective. *IEEE Signal Proc Mag* 35: 82–98. https://doi.org/10.1109/MSP.2017.2785979
20. Bashir Y, bin Waheed U, Ali SH, et al. (2024) Enhanced wave modeling & optimal plane-wave destruction (OPWD) method for diffraction separation and imaging. *Comput Geosci* 187: 105576. https://doi.org/10.1016/j.cageo.2024.105576
21. Bashir Y, Khan M, Mahgoub M, et al. (2024) Machine Learning Application on Seismic Diffraction Detection and Preservation for High Resolution Imaging. International Petroleum Technology Conference, IPTC. https://doi.org/10.2523/IPTC-23668-EA
22. Ishak MA, Islam M, Shalaby MR, et al. (2018) The application of seismic attributes and wheeler transformations for the geomorphological interpretation of stratigraphic surfaces: a case study of the F3 block, Dutch offshore sector, North Sea. *Geosciences* 8: 79. https://doi.org/10.3390/geosciences8030079
23. Brooks C, Douglas J, Shipton Z (2020) Improving earthquake ground-motion predictions for the North Sea. *J Seismol* 24: 343–362. https://doi.org/10.1007/s10950-020-09910-x
24. Pegrum RM, Spencer AM (1990) Hydrocarbon plays in the northern North Sea. *Geo Soc London Special Pub* 50: 441–470. https://doi.org/10.1144/GSL.SP.1990.050.01.27
25. Gautier DL (2005) Kimmeridgian shales total petroleum system of the North Sea graben province. US Geological Survey. https://doi.org/10.3133/b2204C
26. Duin EJT, Doornenbal JC, Rijkers RHB, et al. (2006) Subsurface structure of the Netherlands-results of recent onshore and offshore mapping. *Neth J Geosci* 85: 245.

27. Sørensen JC, Gregersen U, Breiner M, et al. (1997) High-frequency sequence stratigraphy of Upper Cenozoic deposits in the central and southeastern North Sea areas. *Mar Pet Geol* 14: 99–123. https://doi.org/10.1016/S0264-8172(96)00052-9
28. Overeem I, Weltje GJ, Bishop-Kay C, et al. (2001) The Late Cenozoic Eridanos delta system in the Southern North Sea Basin: a climate signal in sediment supply? *Basin Res* 13: 293–312. https://doi.org/10.1046/j.1365-2117.2001.00151.x
29. Kabaca E (2018) Seismic stratigraphic analysis using multiple attributes-an application to the f3 block, offshore Netherlands. University of Alabama Libraries.
30. RIIS F (1992) Dating and measuring of erosion, uplift and subsidence in Norway and the Norwegian shelf in glacial periods. *Nor Geol Tidsskr* 72: 325–331.
31. Qayyum F, Akhter G, Ahmad Z (2008) Logical expressions a basic tool in reservoir characterization. *Oil Gas J* 106: 33.
32. Bijlsma S (1981) Fluvial sedimentation from the Fennoscandian area into the North-West European Basin during the Late Cenozoic.
33. Pauget F, Lacaze S, Valding T (2009) A global approach in seismic interpretation based on cost function minimization. 2009 SEG Annual Meeting, Houston, Texas, 2592–2596.
34. Chopra S, Misra S, Marfurt KJ (2011) Coherence and curvature attributes on preconditioned seismic data. *Leading Edge* 30: 369–480. https://doi.org/10.1190/1.3575281
35. Schmidt I, Lacaze S, Paton G (2013) Spectral decomposition and geomodel Interpretation-Combining advanced technologies to create new workflows. 75th EAGE Conference & Exhibition incorporating SPE EUROPEC 2013, European Association of Geoscientists & Engineers. https://doi.org/10.3997/2214-4609.20130567
36. Imran QS, Siddiqui NA, Latiff AHA, et al. (2021) Automated Fault Detection and Extraction under Gas Chimneys Using Hybrid Discontinuity Attributes. *Appl Sci* 11: 7218. https://doi.org/10.3390/app11167218
37. Hamidi R, Yasir B, Ghosh D (2018) Seismic attributes for fractures and structural anomalies: application in malaysian basin. *Adv Geosci* 2.
38. Hamidi R, Bashir Y, Ghosh DP, et al. (2018) Application of Multi Attributes for Feasibility Study of Fractures and Structural Anomalies in Malaysian Basin. *Int J Eng Technol* 7: 84–87.
39. Sigismondi ME, Soldo JC (2003) Curvature attributes and seismic interpretation: Case studies from Argentina basins. *Leading Edge* 22: 1070–1165. https://doi.org/10.1190/1.1634916
40. Henderson J, Purves SJ, Leppard C (2007) Automated delineation of geological elements from 3D seismic data through analysis of multichannel, volumetric spectral decomposition data. *First Break* 25. https://doi.org/10.3997/1365-2397.25.1105.27383
41. Schroot BM, Schüttenhelm RTE (2003) Expressions of shallow gas in the Netherlands North Sea. *Neth J Geosci* 82: 91–105.